Evaluation of Solar Modelling Techniques through Experiment on a 627kWp Photo-Voltaic Solar Power Plant at Edinburgh College – Midlothian Campus, Scotland.

I Kelly, M Jeffrey, I Smith, and T Muneer

ABSTRACT: The accuracy and applicability of existing methods of solar resource modelling and solar photovoltaic (PV) module performance are investigated in the case of a ground array installation at Edinburgh College, Midlothian Campus, the principal derived quantities consisting of slope irradiation, cell temperature, and cell efficiency. Experimental data were obtained on site through both automated and manual measurements for comparison with the calculated quantities. Results indicate that the horizontal-to-slope conversion models used are extremely accurate, with a greater than 99% degree of confidence in the calculated results. Likewise, correlations between measured and calculated cell temperature were very high at up to 94%. Estimations of the cell efficiency and hence module output were less reliable however, with only one of the models used, for one of the days studied, giving reasonable results. Efficiency values were, however, in the approximately correct range of 15-20%.

1 Introduction

1.1 Solar Energy in Scotland

Solar energy has not traditionally been a focus of investment in Scotland, where the weather is generally considered to be unfavourable and the amount of solar irradiation low. However, a thriving domestic solar market and developing commercial market (examples given below) both indicate that this intuitive judgement may not match the reality. In fact, the average solar resource available in the south of Scotland is only 10% lower than that of middle-England (Rugg, 2012). When factoring in regional variation, some sites in Scotland are likely to be very favourable to solar development indeed.

A critical factor in the swift uptake of solar generation in Scotland and the whole of the UK has certainly been governmental incentivisation, largely through the Renewables Obligation.

The Renewables Obligation (RO) refers to an incentivisation mechanism which was introduced in 2009 and effectively penalises electricity suppliers for failing to source a percentage of their energy from renewable sources (House of Commons, 2012). These percentage targets are met through the purchase of Renewable Obligation Certificates (ROCs) from certified renewable generators. At the end of an accounting year, any shortfall must be paid off into a buy-out fund, which is then divided amongst suppliers who met their targets.

The purpose here is two-fold: on the one hand, suppliers are pressured to conform to government-set (and increasing) targets; on the other, generators are afforded an extra source of income. ROCs were originally issued to suppliers at the rate of 1 per MWh of electricity produced, but now this rate varies with the type of renewable technology.

The equivalent scheme for the small-scale (<50kW) and domestic market is the Feed In Tariff scheme (FIT), introduced in 2010. This is somewhat simpler than the ROCs, in that generators are paid directly for each unit of electricity they generate, and are offered a guaranteed price for any energy they would like to sell. The introduction of the FITs brought about massive uptake in solar systems in the UK, leading to greater production volumes, higher efficiencies and falling system prices (Cherrington, Goodship, Longfield, & Kirwan, 2013). FIT rates were cut dramatically at the end of 2011, leading to a severe slump in the domestic market which is only just starting to recover.

An important point to be noted in the recent changes in solar funding is that government incentives are becoming less critical. Drops in incentives, coupled with dramatic decreases in module and system prices, are making the savings on electricity an increasingly important factor. Martin (Another 5MW solar park to be built for Cornwall, thanks to falling solar prices, 2012) gives the case of a 5MW plant in Cornwall, which was built despite a massive reduction in incentives, simply because capital costs had fallen to the point that the investment was viable even on the reduced incomes.

A specific example of a successful implementation of medium-scale solar is the 15kWp façade-mounted array at Edinburgh Napier University. This system, installed in 2005, produces approximately 9MWh of electrical energy each year, avoiding the use of 1.4 metric tons of carbon (Muneer, Younes, Lambert, & Kubie, 2006). All this with next to zero maintenance or upkeep requirements. Other systems successfully using the power of solar in Scotland include:

- A 150kWp, 792-module array installed on the Malcolm Allen Housebuilders warehouse in Kintore, predicted to generate 114MWh per year (Solar Power Portal, 2012).
- A solar installation of 150kW of solar panels on the roof of the byre at Westerton Farm, Aberdeenshire to reduce the company's dependence on fossil fuels [text removed]. All the solar energy produced is used on

site to power the byre and the milking robots, replacing the dependency on power from the National grid produced by fossil fuels.

2 The Solar Meadow Farm

The solar plant at Edinburgh College, Midlothian Campus, South East Scotland (Figure 1) is a £1.2M, equal-partnership project between Edinburgh College and Scottish & Southern Electricity (SSE) Energy Solutions, who installed and maintain the site. Located in Dalkeith, to the south-east of Edinburgh, the plant was commissioned and built for a number of different purposes: to produce carbon-free, renewable energy, to generate an extra revenue stream for the college, to make good use of previously waste land. For the college, there is also the opportunity to use it as a research and learning environment, where students can get hands-on experience with modern renewable technology. The site has now been made dual-purpose by planting wild meadow-grasses and encouraging the growth of local wildlife, making this plant Scotland's first solar meadow. An area of wetland, and a bank of beehives on the site will further expand the potential ecological benefit to the area.

[Figure 1]

The 627.5kWp installation, as shown in Figure 2, comprises 2,560 solar panels each rated at 230W, 32 P(?) Aurora Power One Trio-20.0-TL [text removed] 20kW inverters and attendant cabling, framing and housing. In fact, over 11km of cable was laid out to connect the AC and DC sides of the system, while almost 1,000 ground screws were planted to support the module mountings. From initial assessments, the site was predicted to produce 568MWh of electrical energy per year, enough energy to power 170 homes. Feeding directly into the National Grid, this energy will offset conventional electricity production to save approximately 293 tonnes of CO_2 per year.

[Figure 2]

The photovoltaic modules used for the plant are ASTRONENERGY Crystalline PV Module CHSM6610P Series. The Polycrystalline modules have a nominal power output of 230W, with an overall module efficiency of 14%. Modules are connected in series strings of 20 modules each, with 4 parallel strings per inverter. The Power-One Aurora Trio inverters each have a maximum power input of 20kW and a nominal efficiency of 98%. The modules are mounted on framing orientated due south, with an inclination of 25° degrees.

While the site has now been completed, and in fact started producing on the 28/03/2013, contractual details have only recently been worked out. This proved problematic for the completion of this project, and for the College in general, as the site and data access were not always available.

There were a number of issues to overcome in the first year of operation. Initially 6 out of the 32 inverters were not available for the parallel connection, thus preventing maximum yields for the first 2 months of operation. This limiting effect resulted in the inverters only being able to operate at 12kW instead of the 20kW expected, i.e. these inverters were only operating at 60% of their maximum input power. Additionally, a problem with transformer balancing and variable phasing issues caused the substation to trip out on the Solar Meadow side. This has meant that a total of 4-5 weeks generation have been lost. Both of these factors have contributed to a shortfall in production during year 1 of operation. By May 2014 440MWh of power had been generated, compared to the initial estimate of 568MWh. This corresponds well, however, against a revised, SAP projection of 431MWh which included reduction due to shading as well as the aforementioned downtime. Subsequently, further works have been carried out to install fans and heatsinks to all the inverters to increase heat dissipation and the transformer taps have been changed on the national grid side to lower the operating level to a point where phase shifts and grid fluctuations will have less impact at peak times.

3 Shading Analysis

In the first stage of the project, a site survey was undertaken. This was done in order to ascertain what measures were required to complete the later experimental work, to ensure the reference documents such as site plans and electrical connections were accurate, and also to determine what shading, if any, was present on the site.

Shading is an important factor in the operation of any solar installation, as it not only cuts down on the solar energy available to the system to be converted to electrical output, but also interferes with system operation: one shaded module can affect the performance of an entire string. [add reference to shading resource?]

[Figure 3]

A basic shading analysis was undertaken at 5 points (figure 3) toward the south end of the site where shading effects are more severe. The main obstacles to be considered were the tree lines to the south-east and south-west, and the earth wall enclosing the site. Elevations and positions were derived from both the site plan, and measurements taken by theodolite. These elevations were then used to construct horizon lines for each point. Examples are shown in Figures 4 and 5.

[Figure 4]

[Figure 5]

The shading analysis indicates that a significant portion of incident radiation will be lost to shading effects for the southern-most rows of modules. This shading will be more serious in the afternoon for the southerly points, and in the morning for the easterly points.

4 Experimental Measurements at Solar Meadow Farm

Experimental data was collected at the site to fulfil two goals. Firstly to obtain detailed, specific data on the day-to-day operation of the plant, and secondly to assess the accuracy of solar models used to predict such values as in-plane (or slope) irradiation, PV module cell temperature, and cell efficiency.

The experimental setup consisted of the following:

- heat flux sensors mounted directly on the back panel of one of the PV modules. These were used to determine the rate of heat transfer between the module and its surrounding.
- K-type thermocouples. Two of these were mounted in a similar way to the heat flux sensors to determine cell temperature, while another two were used to record air temperature under shade.
- solar pyranometers. These were mounted on tripods: one above the modules facing directly upwards to record the horizontal solar irradiation, and two in the plane of the modules (with equal inclination and orientation) to record the slope irradiation.
- Two data-loggers, which the sensors were wired into and which recorded 5-minute periodic averaged values of the sensor outputs.

The sensors were positioned around the solar modules as shown in Figures 6 & 7.

[Figure 6]

[Figure 7]

Data from each of the temperature, flux and irradiation sensors was logged using two Grant 2020 series ‘Squirrel’ data-loggers, taking measurements every 5 minutes across the day. These data points constituted the average value (temperature, irradiation or heat flux) registered over the 5-minute period, forming the basis for the calculation process.

The final data values needed were the power output of the solar module being measured. Unfortunately, no method of automated logging of module output was available, and a compromise had to be made. Manual readings from

the string inverter corresponding to the chosen PV module were taken, over the course of three days. The module output was simply estimated as a fraction (1/80) of the input power to the inverter.

5 Calculation Process

The comparison of measured and calculated variables was completed according to Figure 8.

[Figure 8]

This being a linear calculation process, each stage relying on the previous, any errors or inaccuracies picked up would be propagated through the calculations, making an accurate, independent assessment of each stage difficult. For this reason, calculations were based on measured data along with previous-stage calculated values at every opportunity.

5.1 Slope Irradiation

As indicated in Figure 8, the principal input variables to determine the slope irradiation (once the position of the slope has been decided) are the horizontal irradiation and the time of day (and date), which allow the position of the sun in the sky to be calculated. As data readings were taken over 5 minute time intervals, not at an exact time, it was decided to follow the approach used by Clarke, et al. (2007) and take the mid-point of the time period as the data point, ie. 2.5 minutes before the logged time.

Figure 9 shows how the time/date and irradiation data were used with solar geometry equations. One source that may be used for such analysis is Muneer (2004).

[Figure 9]

The final important factor to be determined was the diffuse irradiation component, ie the solar energy emitted across the whole hemisphere of the sky rather than directly from the sun. This was achieved through use of separate models for relating the relationship between the global clearness index $k_t = I_G/I_E$, and the horizontal diffuse to global ratio $k = I_D/I_G$. (Where I_G is the global irradiation and I_D the diffuse).

This relationship allows us to calculate the diffuse irradiation, rather than directly measure it, which is a critical step towards determining the slope irradiation.

Three different equations (5.1, 5.2, and 5.3) were selected to generate a range of results, one from Muneer et al. (2000), the others from Clarke et al. (2007). They are shown below with coefficients selected for Edinburgh:

$$k = 0.8721 + 1.7619k_t - 6.2135{k_t}^2 + 3.9467{k_t}^3$$

$$for\ k_t < 0.25, k = 1$$

$$for\ k_t > 0.8, k = 0.3$$

Equation 5.1: Clarke Seasonal (Summer) Calculation, Source (Clarke, Munnawar, Davidson, Muneer, & Kubie, 2007)

$$k = 0.8798 + 1.7195k_t - 6.1193{k_t}^2 + 3.8769{k_t}^3$$

$$for\ k_t < 0.2, k = 0.98$$

$$for\ k_t > 0.85, k = 0.3$$

Equation 5.2: Clarke June Calculation, Source: (Clarke, Munnawar, Davidson, Muneer, & Kubie, 2007)

$$k = 1.006 - 0.317k_t + 3.1241{k_t}^2 - 12.7616{k_t}^3 + 9.7166{k_t}^4$$

Equation 5.3: Muneer Calculation, Source: Software Program Calc4-08 in (Muneer, Abodahab, Weir, & Kubie, 2000)

Once both the diffuse and global (total) horizontal irradiation are known, it becomes possible, for a given collector inclination and orientation, to calculate the global slope irradiation (generally referred to as the slope irradiation). This method is adapted directly from the Windows in Buildings (Muneer, Abodahab, Weir, & Kubie, 2000) software. Three quantities are calculated separately for the plane of the collector:

- beam irradiation
- diffuse irradiation
- ground-reflected irradiation

Beam irradiation depends on the global and diffuse horizontal irradiation, the angle of the Sun's angle of incidence on the centre of a solar panel (SOLINC) and the Sun's Altitude as seen in the sky above a solar panel (SOLALT). It is set to zero if either SOLALT is less than 7°, or SOLINC is greater than 90°. In other words, if the sun is not in 'view' of the collector. Otherwise, the beam component is given by (equation **5.4**):

$$Beam_{slope} = Beam_{horizontal}\frac{\cos SOLINC}{\sin SOLALT}$$

Equation 5.4: Beam Component of Slope Irradiation, Source: Software Program Calc4-08 in *(Muneer, Abodahab, Weir, & Kubie, 2000)*

Diffuse slope irradiation is more complex to determine, as in the model proposed by Muneer (2004), the sky is not considered isotropic. This method has been shown to give better results for diffuse irradiation (Muneer 2004). Complete algorithmic details for the calculation of the above mentioned slope irradiation and computations are provided in the latter reference. The final value used for the slope irradiation during the given time period is simply the sum of the beam, diffuse and ground-reflected components.

5.2 Cell Temperature

The cell temperature, similarly to the slope irradiation, was estimated through the use of three different models. The NOCT model is based on the behavior of a solar module under certain test conditions, and utilises a simple calculation relating the solar irradiation to the temperature (equation **5.5**):

$$T_c = T_a + \frac{G_{slope}}{G_{noct}}\left(T_{c,noct} - T_{a,noct}\right)\left(1 - \frac{\eta_{stc}}{\tau\alpha}\right)$$

Equation 5.5: NOCT Cell Temperature Calculation

Where: T_c is the cell temperature, T_a is the air temperature, G_{slope} is the global slope irradiation, G_{noct} equals 800W/m^2, $T_{c,noct}$ and $T_{a,noct}$ are the cell and air temperatures at NOCT, η_{stc} indicates the cell efficiency at STC (standard test conditions) and $\tau\alpha$ is related to the absorptivity of the module to light.

The HOMER software model alters equation **5.5** to include a linearly variable, rather than static cell efficiency (equation **5.6**).

$$T_c = \frac{T_a + \left(T_{c,noct} - T_{a,noct}\right)\frac{G_{slope}}{G_{noct}}\left[1 - \frac{n_{stc}\left(1 - \alpha_p T_{c,stc}\right)}{\tau\alpha}\right]}{1 + \left(T_{c,noct} - T_{a,noct}\right)\frac{G_{slope}}{G_{noct}}\frac{\alpha_p n_{stc}}{\tau\alpha}}$$

Equation 5.6: HOMER Cell Temperature, Source: (HOMER Energy, 2013)

In the third case, a thermal model was implemented based on the method proposed in Aldali, et al. (2013). This avoids the assumption of the previous methods: that the module's thermal parameters will not change under different circumstances such as air temperature or irradiation.

[Figure 10]

In Figure 10, it can be seen that there are three main mechanisms for thermal energy transfer from the cell (or module) to its surroundings. These correspond to convective losses to the air on both sides of the cell, and radiative losses to the sky (radiative losses to the ground are much smaller, and are neglected).

The convective losses are a function of the temperature difference between cell and air (equation 5.7):

$$Convective\ Loss = 2h_{ca}(T_c - T_a)$$

Equation 5.7: Convective Loss

The radiative losses likewise, but to the sky (equation 5.8):

$$Radiative\ Loss = h_{cs}(T_c - T_{sky})$$

Equation 5.8: Radiative Loss

In which T_{sky}, the effective sky temperature, and h_{ca} and h_{cs} can be determined from equations 5.9, 5.10 and 5.11:

$$T_{sky} = 0.0552{T_a}^{1.5}$$

Equation 5.9: Effective Sky Temperature, Source: (Aldali, Celik, & Muneer, 2013)

$$h_{ca} = 5.67 + 3.8v$$

Equation 5.10: Air Heat Transfer Coefficient, Source: (Aldali, Celik, & Muneer, 2013)

$$h_{cs} = \frac{\sigma\varepsilon_c({T_c}^4 - {T_{sky}}^4)}{T_c - T_{sky}}$$

Equation 5.11: Sky Heat Transfer Coefficient, Source: (Aldali, Celik, & Muneer, 2013)

The cell temperature value is found by combining the energy losses with the heating effect from the sun (equation 5.12):

$$T_c = \frac{I_{slope}\tau\alpha(1 - \eta_{cell}) + h_{cs}T_{sky} + 2h_{ca}T_a}{h_{cs} + 2h_{ca}}$$

Equation 5.12: Thermal Model Cell Temperature

Where: I_{slope} is the incident irradiation. The value for T_c is derived iteratively as T_c affects the heat transfer coefficients h_{cs} and h_{ca}.

5.3 Cell Efficiency

While the other variables could be measured fairly directly, the cell efficiency had to be estimated from the measured data (using equation 5.13).

$$Cell\ Efficiency = \frac{P_{out}}{P_{in}} = \frac{{P_{module}}/{No.of\ Cells}}{Solar\ Irradiation \times Cell\ Area}$$

Equation 5.13: Cell Efficiency from Output

P_{module} was derived from the manually-recorded inverter power readings at each time interval. This was done in two ways to get the best possible result: first of all as an average of a set of instant power readings taken around the sample time, and secondly from the change in total inverter energy reading over the time period, divided by the sample time. Each reading had its own advantages. In general, the instant readings were more highly variable, whereas the averaged readings were adversely affected by the low resolution of the energy counter (nearest 0.1kWh).

$$\eta_{cell} = \eta_{stc}[1 + \alpha_p(T_c - T_{c,stc})]$$

Equation 5.14: Cell Efficiency

$$\eta_{cell} = \eta_{stc}[1 + \alpha_p(T_c - T_{c,stc}) + \gamma \log \phi]$$

Equation 5.15: Cell Efficiency with Irradiation, Adapted from (Mattei, Notton, Cristofari, Muselli, & Poggi, 2006)

Equations 5.14 and 5.15 were both used as models for the cell efficiency, based on (in both cases) cell temperature and (in the second case only) irradiation.

6 Results & Discussion

6.1 Slope Irradiation

The measurement of slope irradiation was relatively simple and reliable, as the use of a professionally calibrated pyranometer aligned to match the slope and orientation of the solar module in question gave accurate readings with which to check the calculated values against. More complex was the method used for calculating the slope irradiation from only the horizontal global irradiation, requiring a number of different steps and intermediate quantities (as covered in Section 5.1); regardless it was expected that the calculation accuracy would be relatively high, as has been demonstrated in the papers presenting the methods used (Aldali, Celik, & Muneer, 2013) (Clarke, Munnawar, Davidson, Muneer, & Kubie, 2007).

The three models for determining the clearness index and hence the slope irradiation gave similar results, the best of which is shown in Figure 11, derived from the Clarke Summer model.

[Figure 11]

It can be seen that Figure 11 shows an excellent, almost entirely linear, correlation for the site studied.

While all three methods show a high degree of accuracy, as expected the calculations optimised for the given location give slightly better results. Table 1 makes a direct comparison in terms of the same quantities highlighted

in the Figure 11: gradient, y-axis intercept and regression coefficient, R^2, between the computed and measure quantities.

[Table 1]

The difference between using the seasonal and monthly models follows the assessment in Clarke et al. (2007), namely that the increased complexity of using monthly coefficients (as in the June model) in a project gives a low return in increased accuracy (in this case, little to none).

6.2 Cell Temperature

As detailed in Section 5.2, the cell temperature was modelled in three ways; the simple but widely-used NOCT or nominal operating cell temperature model, the slightly more complex one used in the HOMER software, and finally the full thermal model. It was expected that each would give successively better results when compared with the cell temperature directly measured from the back of the PV module, with the thermal model being significantly more accurate than the other two due to its consideration of a greater number of factors. Figure 12 shows the output of the thermal model only across the full time range of the experiment, while Table 2 compares the outputs of the three models.

[Figure 12]

[Table 2]

These results clearly show the relatively high reliability of the simple NOCT method. Comparing the three methods, we can see the reliability (or R^2 value) of every method is around 94%, with the HOMER software calculation performing very slightly better than the others. A larger difference can be seen in the gradient, which indicates the average percentage error if we utilise the given method of calculation. Here, the thermal model gives the best results, corresponding to only a 1.5% degree of error compared to 6.6% for the NOCT model and 11.3% for the HOMER model.

It is proposed that with the inclusion of reliable and high-resolution wind data, the thermal model could be optimised to give even better results than it has done, particularly at higher temperatures when the measured value starts to vary further from that calculated.

6.3 Cell Efficiency

The cell efficiency differed from the other two quantities since it is not a directly-measured quantity; Efficiency is derived from the power in to and useful power out from a system, in this case solar irradiation and electrical power.

Since automatic logging of electrical power was not possible as part of the experiment and manual measurements had to suffice, two problems arose: which method of determining the average power value for the time period to use (as described in Section 5.3) and assuring accuracy in the timing of measurements.

The calculated cell efficiency, derived from the two equations given in Section 5.3, was compared with the efficiency value estimated from both the averaged and instantaneous power readings taken manually. Two example days are shown in Figures 13 and 14.

[Figure 13]

[Figure 14]

As can be seen in Figure 13, a very low correlation is observed between the calculated and measured (estimated) values during a cloudy day. This is largely due to the fast changes in both irradiation and cell temperature with time, and the use of manually-recorded (and time-inaccurate) measurements. On the other hand, a fairly good correlation is seen over the course of a clear day (Figure 14). Here, any changes in efficiency are gradual, reducing the importance of the time component.

The range over which the cell efficiency varied was approximately correct, although the calculated value exhibited greater variability than the measured (estimated) values.

[Figure 15]

Figure 15 shows the efficiencies measured from both the instant and period-average power readings, along with that calculated from equation 5.18. All three show an average value of close to 16%. As would be expected, the instant-based readings vary more widely than the period-average readings. The calculated values stray even further than this, however. This would imply that the formula used is too sensitive to variable input, and that in fact the coefficients should be smaller. One possible cause is a high estimate of the power temperature coefficient of the solar module, as obtained from the ASTRONENERGY module datasheet. This may be due to safe-side estimation. Hmm, so this isn't true – I thought the modules were CSUN.

6.4 System Performance

As covered previously, the initial estimated generation of the solar meadow farm as produced by SSE was 568,611kWh over a full year's operation. This is a significant amount of power, avoiding the production of 293,000kg of CO_2. On the 4th September 2013 a generation meter reading of 283,021kWh was taken by SSE engineers, which

seemed to correspond fairly well to prediction, as this was covering the months April-August only. The total produced by the end of year 1, however, turned out to fall short at 439,276kWh. When taking the revised SAP estimation of X kWh, including a reduction for shading of 8,566kWh and a further reduction for system downtime of X kWh, the system can be said to be operating well outside of the problems covered in section 2.

The solar meadow farm at Edinburgh Midlothian campus is more than just a valuable financial investment, it is a firm indication of the viability and importance of large-scale solar in Scotland. It supports the strong likelihood of the future uptake of projects of this kind as part of a greener, more sustainable energy solution.

7 Conclusions

The performance of a range of solar and solar module models have been assessed through a study done on a commercial solar plant in the Edinburgh area. An experiment to measure a range of data quantities was designed and implemented, and a survey of the site to obtain an estimate of the degree of shading was performed. To overcome limitations on data available to the researcher, three days of manually-recorded measurements were made to support the experimental data.

The shading characteristic of the site was not assessed in a great degree of detail, but it was clearly shown that the figure of zero shading for the site assumed by the contractors would prove to be inaccurate, particularly in the winter months. This was borne out by the revised SAP site assessment. Shading was shown to be most severe at the southern end of the site, and still notable along the eastern side. Any shading on the solar modules adversely affects the performance of the entire string in question, having a disproportionately large effect on plant output.

The conversion of solar irradiation data from horizontal intensity to intensity received on a slope has been shown to be extremely accurate when using location-specific regression formulae. It was concluded that the seasonal model proposed by Clarke et al (2007) proved the most accurate of those considered over the recorded time period, by a small margin. A further advantage of the given method is the slightly simpler implementation compared to the monthly model, which requires a different set of regulated coefficients to be used for every month.

The prediction of a solar photovoltaic module's cell temperature from environmental data such as air temperature and solar irradiation was shown to be fairly accurate and reliable across three different calculation methods. The simplest, based on the 'nominal operating cell temperature' of the module, actually gave results almost as good as the much more complex thermal model, indicating that this is a reliable and useful method to use. The thermal model was assumed to be limited by the lack of good quality, high resolution wind data for the site studied. In addition, the range of assumed input variables requires better definition.

Finally, the calculation of cell efficiency over the three days of manual data recordings was performed, giving mixed results. Due to large uncertainties in the actual value, coupled with the small efficiency range, results were relatively inconclusive. The difficulty encountered was whether to ascribe the poor quality of results to the models used, or the data collected. The one exception, on a clear-sky day when the related uncertainties were small, indicated that with reliable, automatically logged power data the models used could yield much more favourable results. On the other hand, the approximate cell efficiency was adequately predicted, in as far as lying between 12-18% and being generally lower on hotter days, or in the afternoon.

The implementation of more accurate and high-resolution data collection methods on the site in the future, currently under discussion, will open up excellent opportunities for further analysing and improving the results of this investigation.

8 Acknowledgments

…

9 References

Aldali, Y., Celik, A., & Muneer, T. (2013). Modeling and Experimental Verification of Solar Radiation on a Sloped Surface, Photovoltaic Cell Temperature, and Photovoltaic Efficiency. *Journal of Energy Engineering, 139*(1), 8-11.

Cherrington, R., Goodship, V., Longfield, A., & Kirwan, K. (2013). The feed-in tariff in the UK: A case study focus on domestic photovoltaic systems. *Renewable Energy, 50*, 421-426.

Clarke, P., Munnawar, S., Davidson, A., Muneer, T., & Kubie, J. (2007). Technical note: An investigation of possible improvements in accuracy of regressions between diffuse and global solar irradiation. *Building Services Engineering Research and Technology, 28*(2), 189-197.

Grassie, T. (2012). Autonomous Wind/PV Hybrid System Sizing, lecture notes distributed in the topic MEC11123-Sustainable Energy Technologies. Napier University,: Edinburgh on 21st November.

HOMER Energy. (2013). *HOMER Software*. Retrieved August 19, 2013, from http://homerenergy.com/software.html

House of Commons. (2012). *The Renewables Obligation*. Retrieved August 19, 2013, from www.parliament.uk/briefing-papers/sn05870.pdf

Martin, J. (2012, September 11). *Another 5MW solar park to be built for Cornwall, thanks to falling solar prices.* Retrieved August 19, 2013, from http://www.solarselections.co.uk/blog/one-more-5mw-solar-park-for-cornwall

Mattei, M., Notton, G., Cristofari, C., Muselli, M., & Poggi, P. (2006). Calculation of the polycrystalline PV module temperature using a simple method of energy balance. *Renewable Energy, 31*, 553-567.

Muneer, T. (2004). *Solar Radiation and Daylight Models* (2nd ed.). Oxford: Elsevier Butterworth-Heinemann.

Muneer, T., Abodahab, N., Weir, G., & Kubie, J. (2000). *Windows in Buildings: Thermal, Acoustic, Visual and Solar Performance* (1st ed.). Oxford: Butterworth-Heinemann.

Muneer, T., Younes, S., Lambert, N., & Kubie, J. (2006). Life cycle assessment of a medium-sized photovoltaic facility at a high latitude location. *Proc. IMechE Vol 220 Part A: J. Power and Energy*, 517-524.

Rugg, P. (2012). *Renewable Energy Planning Guidance Note 2: The development of large scale (>50kW) solar PV arrays*. Retrieved August 19, 2013, from http://www.solar-trade.org.uk/media/2%20Large%20Scale%20Solar%20PV%20%20August%202012.pdf

Solar Power Portal. (2012, September 11). *Malcolm Allen Housebuilders invest in one of Scotland's largest solar arrays.* Retrieved from Solar Power Portal Website: http://www.solarpowerportal.co.uk/case_studies/malcolm_allen_housebuilders_invest_in_one_of_scotlands_largest_solar_2356

UO Solar Radiation Monitoring Laboratory. (2007). *Sun path chart program*. Retrieved August 19, 2013, from http://solardat.uoregon.edu/SunChartProgram.html

List of Figures

Fig 1: Midlothian Solar Meadow Farm

Fig 2: Site Plan of the Meadow

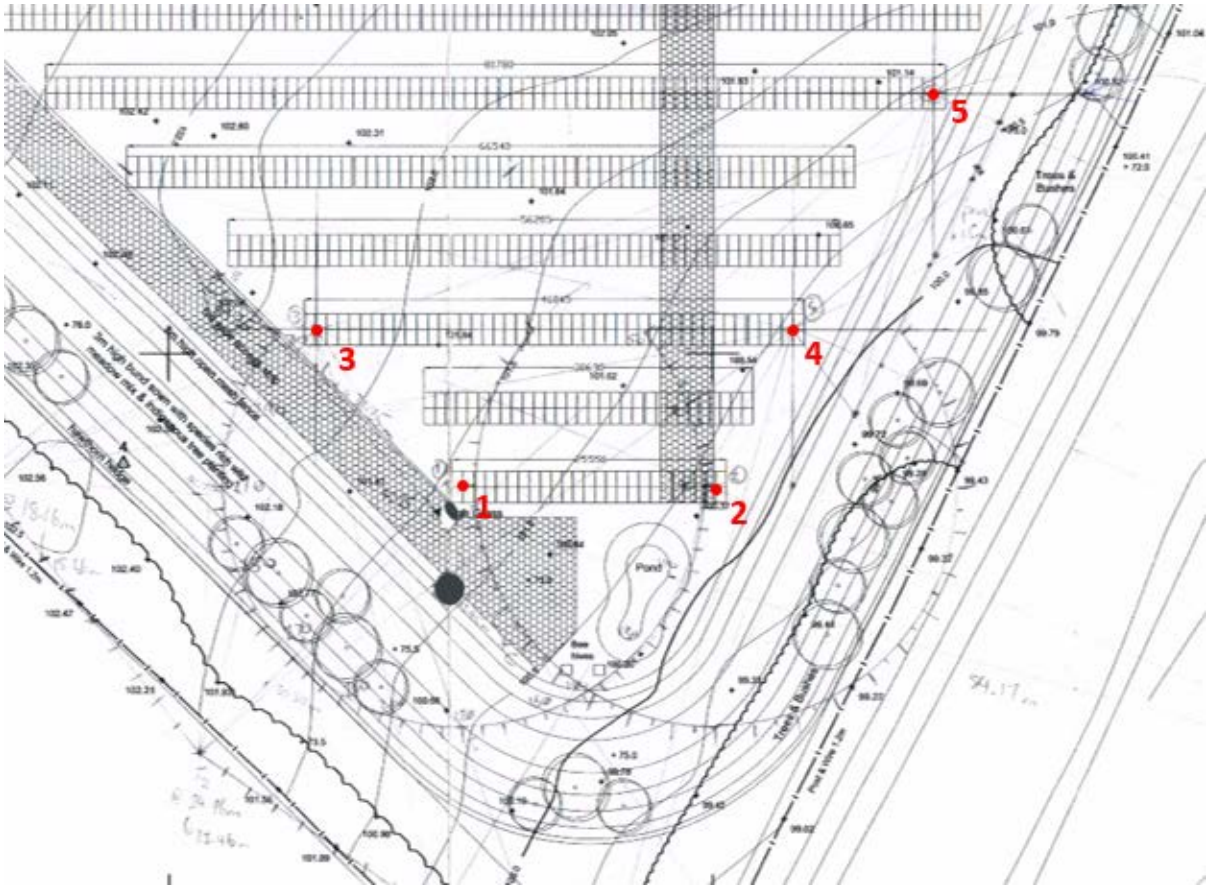

Fig 3: Shading Analysis Locations (based on figure 2)

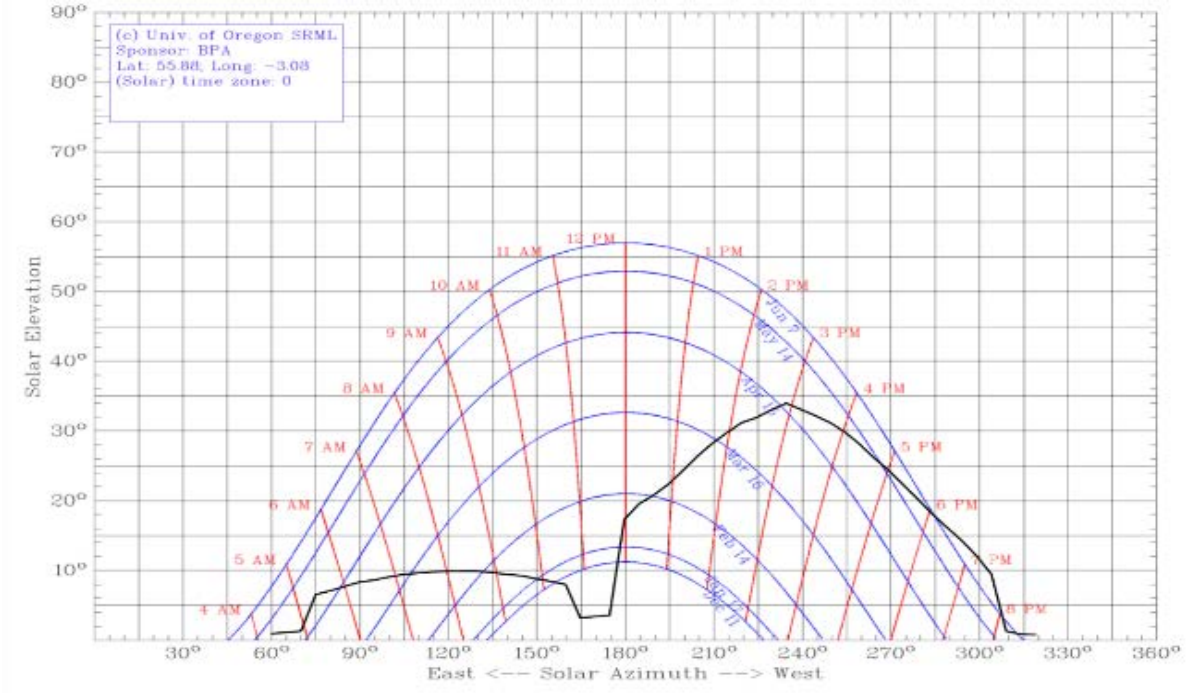

Fig 4: Shading at Point 2

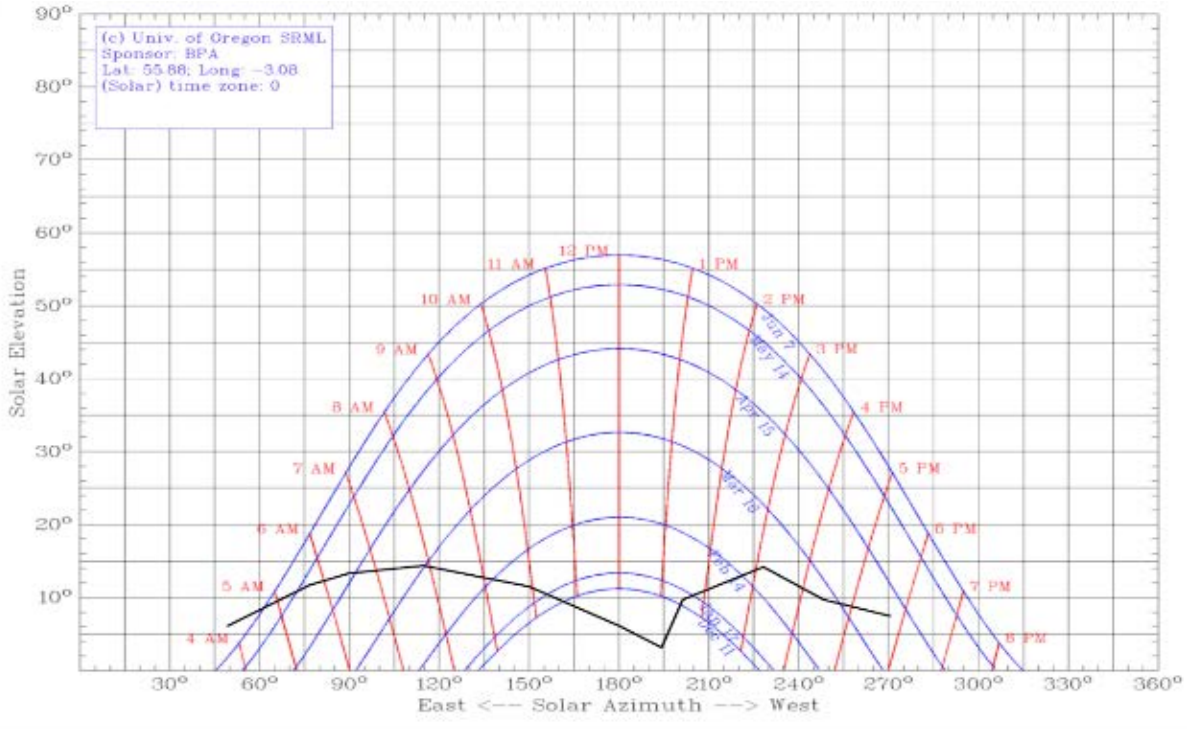

Fig 5: Shading at Point 5

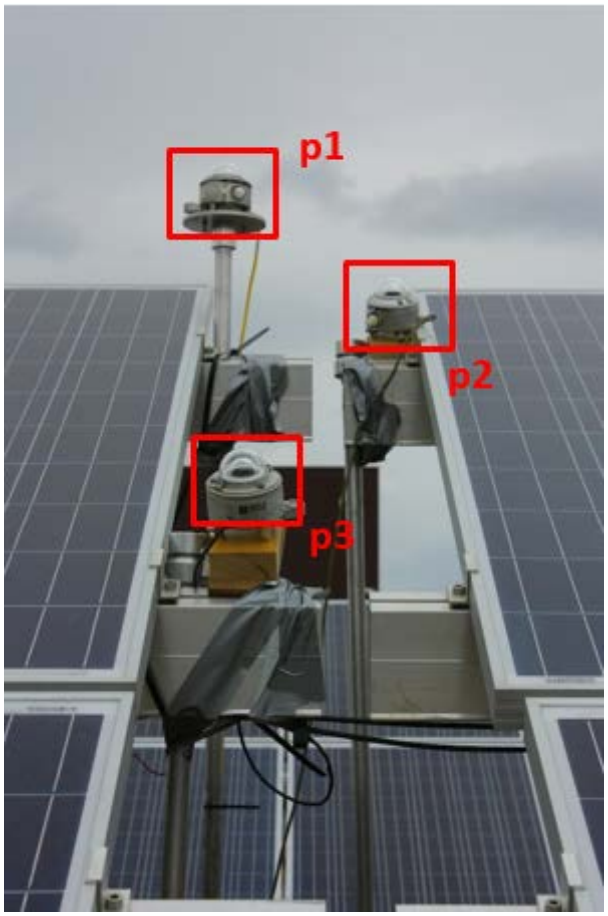

Fig 6: Position of Pyranometers

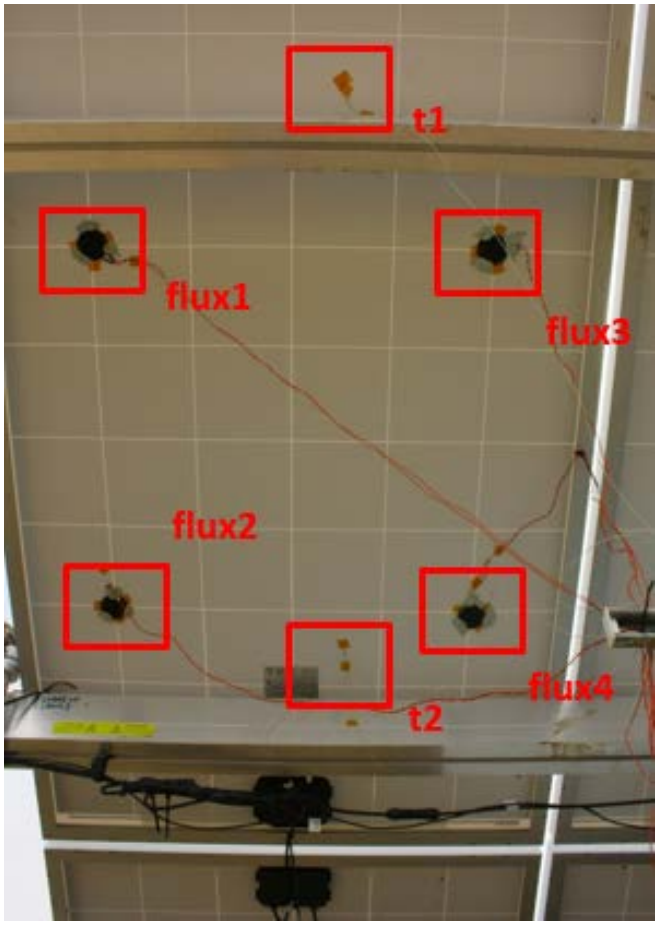

Fig 7: Position of Flux Sensors

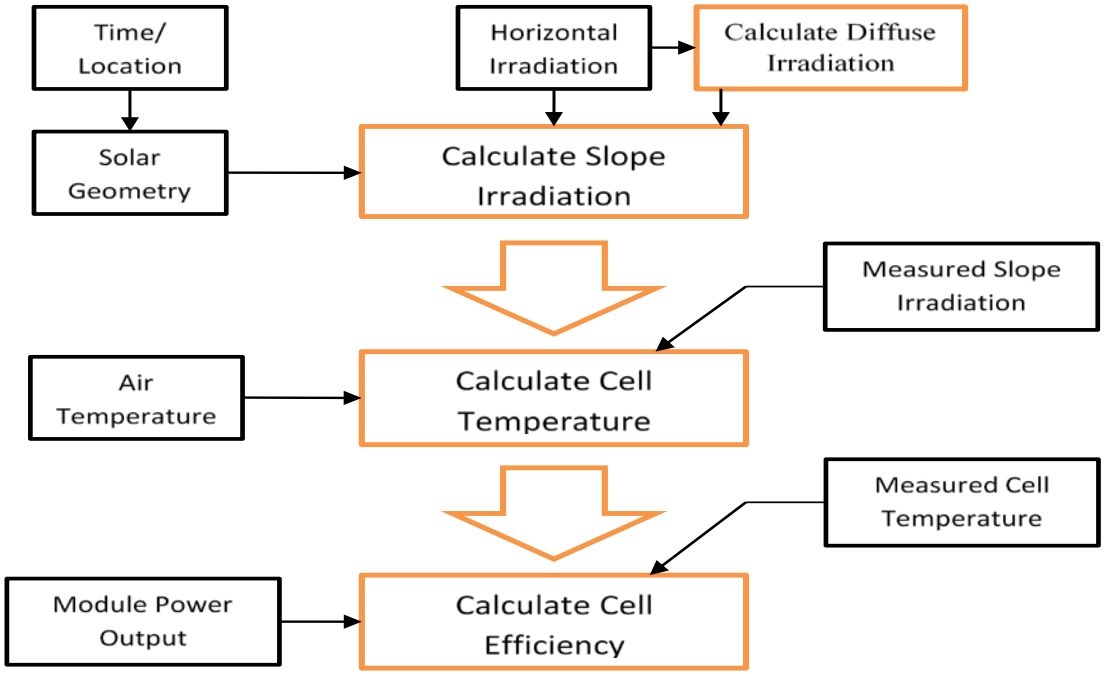

Fig 8: Calculation Flow Chart

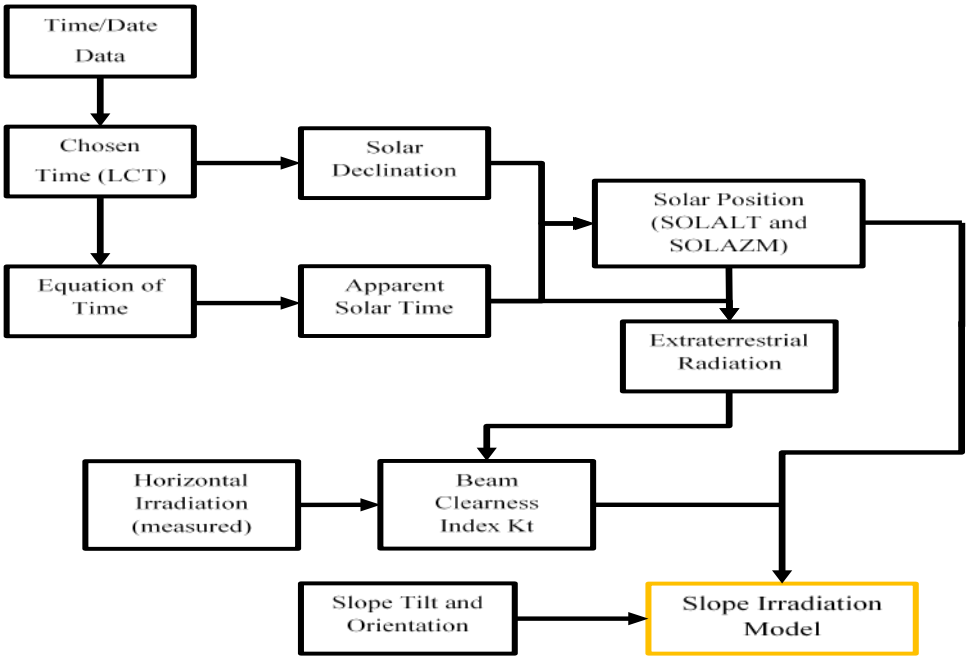

Fig 9: Solar Geometry and Slope Irradiation

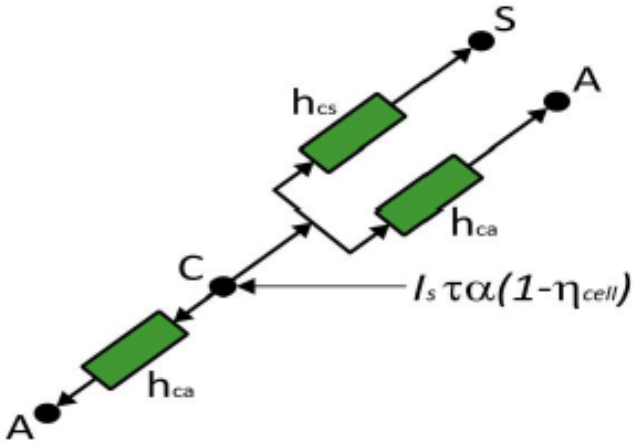

Fig 10: Heat Transmission from a Solar Module, Source: (Aldali, Celik & Muneer, 2013)

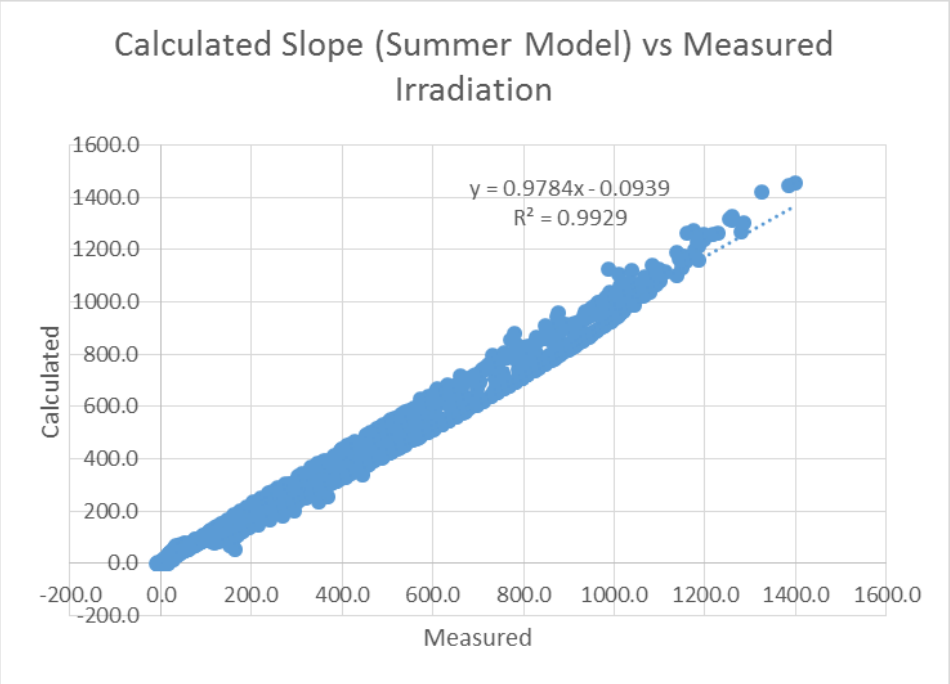

Fig 11: Slope Irradiation Results

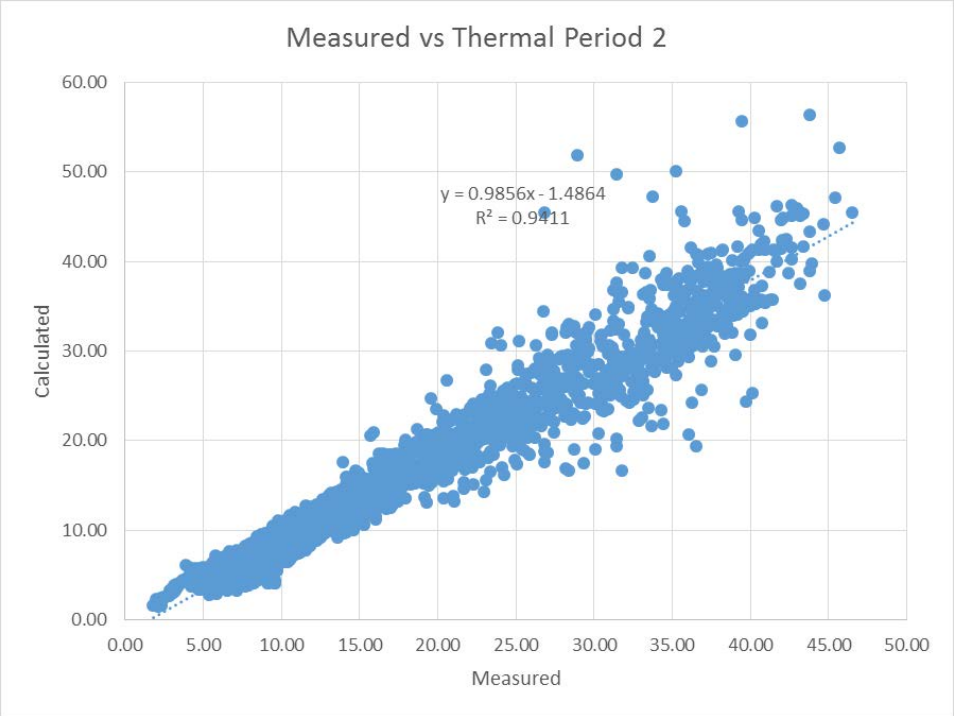

Fig 12: Cell Temperature Results

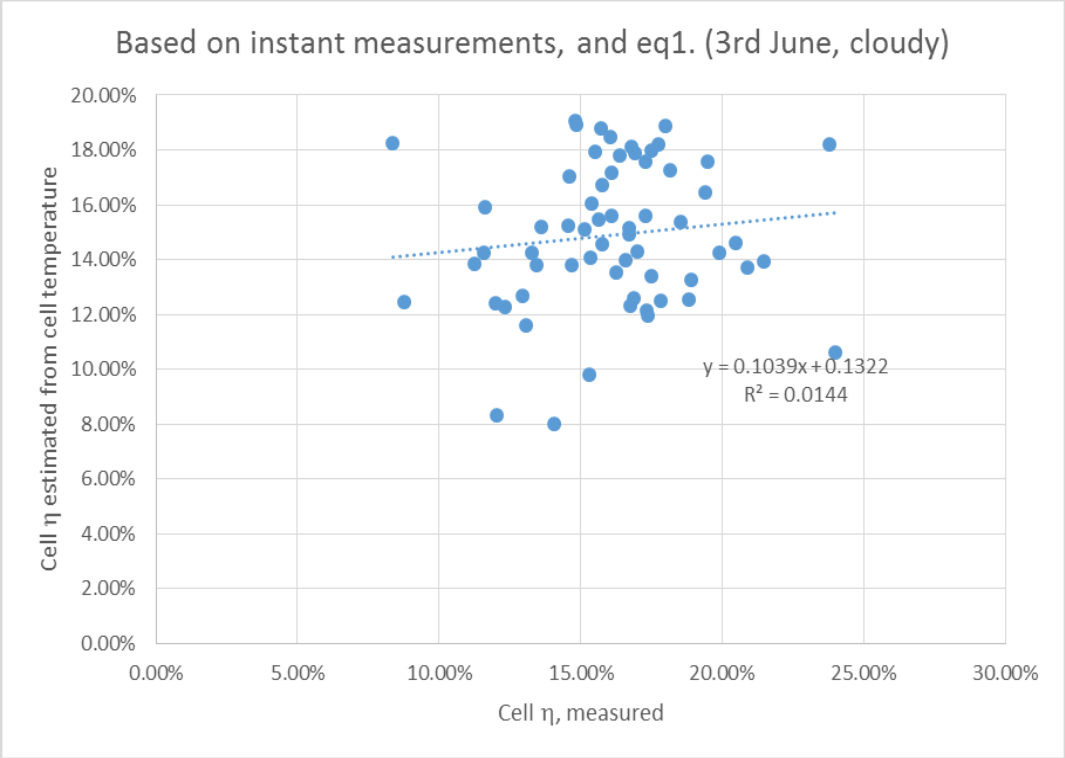

Fig 13: Cloudy-Day Efficiency

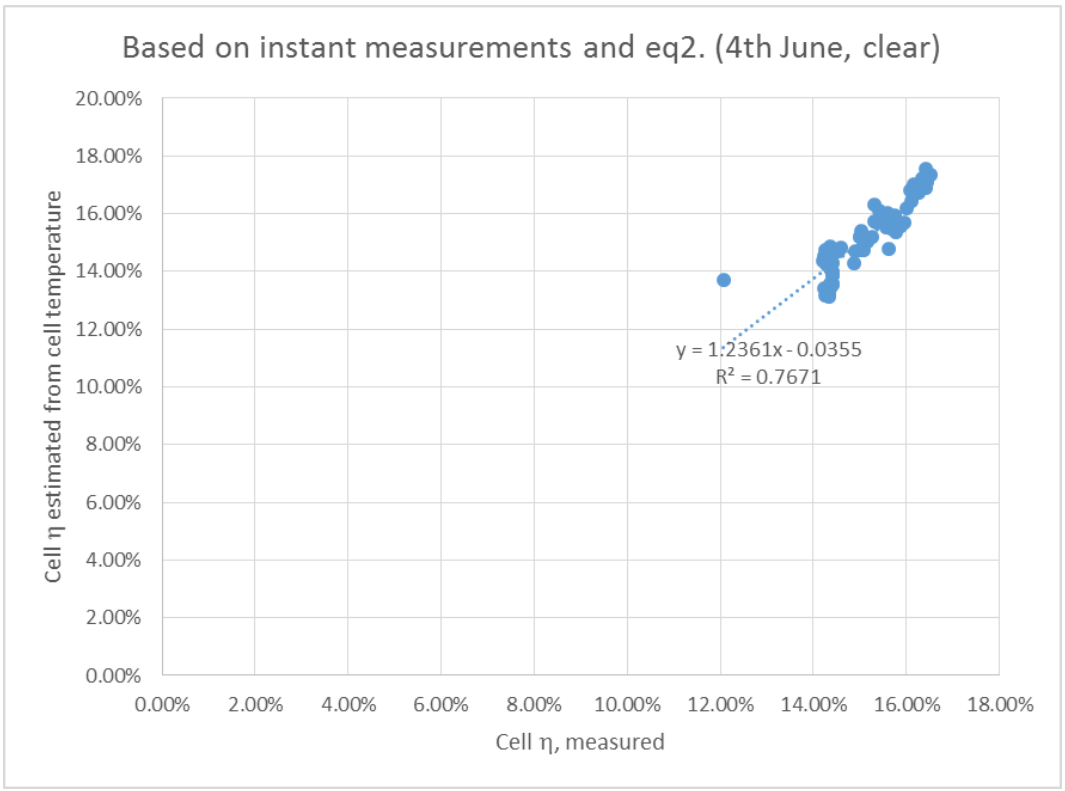

Fig 14: Clear-Day Efficiency

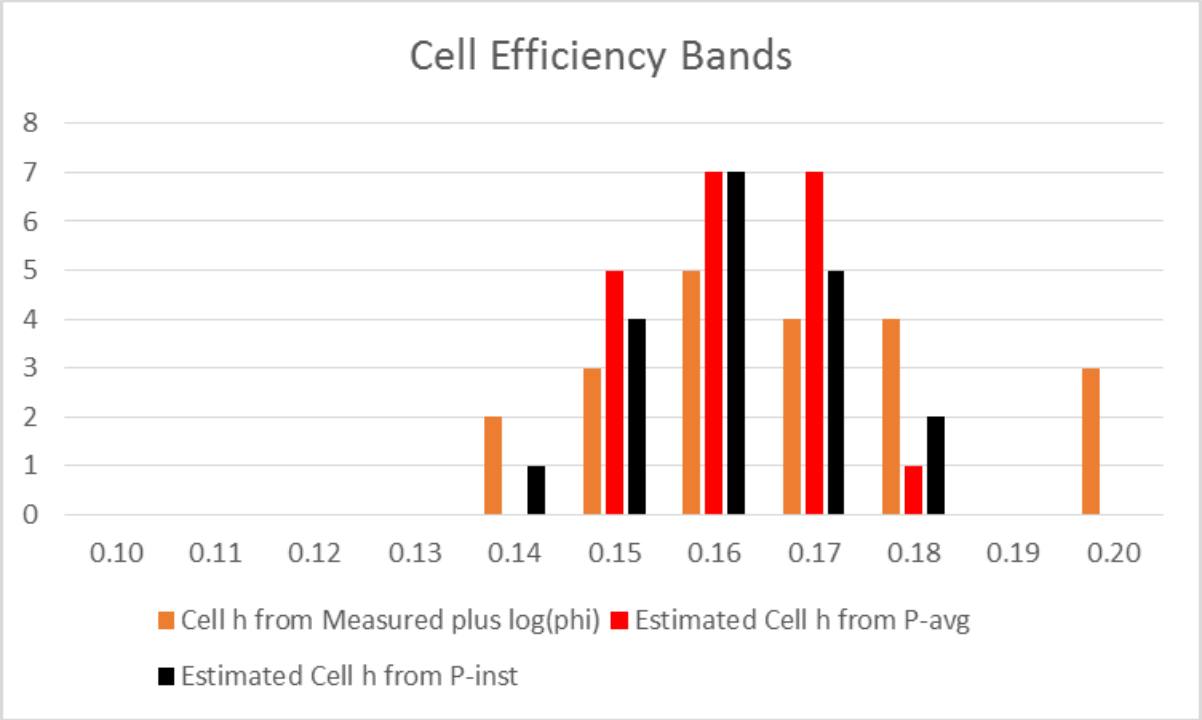

Fig 15: Cell Efficiency Bands

List of Tables

Slope Irradiation Comparison			
Model	**Gradient**	**Offset**	**R^2**
Summer	0.9784	0.0939	0.9929
June	0.9761	0.3164	0.9929
Muneer	0.9738	0.405	0.9897

Table 1: Slope Irradiation Model Results

Cell Temperature Comparison			
Model	**Gradient**	**Offset**	**R^2**
NOCT	1.0662	0.7332	0.9401
Homer	0.8876	2.303	0.9452
Thermal	0.9856	-1.4864	0.9411

Table 2: Cell Temperature Model Comparison